

## Laser irradiation-induced $\alpha$ to $\delta$ phase transformation in Bi<sub>2</sub>O<sub>3</sub> ceramics and nanowires

M. Vila, C. Díaz-Guerra, and J. Piqueras

Citation: *Appl. Phys. Lett.* **101**, 071905 (2012); doi: 10.1063/1.4747198

View online: <http://dx.doi.org/10.1063/1.4747198>

View Table of Contents: <http://apl.aip.org/resource/1/APPLAB/v101/i7>

Published by the AIP Publishing LLC.

---

### Additional information on Appl. Phys. Lett.

Journal Homepage: <http://apl.aip.org/>

Journal Information: [http://apl.aip.org/about/about\\_the\\_journal](http://apl.aip.org/about/about_the_journal)

Top downloads: [http://apl.aip.org/features/most\\_downloaded](http://apl.aip.org/features/most_downloaded)

Information for Authors: <http://apl.aip.org/authors>



# Laser irradiation-induced $\alpha$ to $\delta$ phase transformation in $\text{Bi}_2\text{O}_3$ ceramics and nanowires

M. Vila, C. Díaz-Guerra,<sup>a)</sup> and J. Piqueras

Departamento de Física de Materiales, Facultad de Ciencias Físicas, Universidad Complutense de Madrid, Ciudad Universitaria s/n, 28040 Madrid, Spain

(Received 18 May 2012; accepted 3 August 2012; published online 16 August 2012)

The  $\alpha$ - $\text{Bi}_2\text{O}_3$  to  $\delta$ - $\text{Bi}_2\text{O}_3$  phase transformation has been locally induced by laser irradiation in ceramic samples and single-crystal nanowires of this oxide. The threshold power densities necessary to induce this transformation, as well as the corresponding transformation kinetics and its temporal stability, have been investigated in both kinds of samples by micro-Raman spectroscopy. The appearance of the  $\delta$  phase was also monitored by spatially resolved photoluminescence spectroscopy. An emission band peaked near 1.67 eV, not observed in  $\alpha$ - $\text{Bi}_2\text{O}_3$ , is tentatively attributed to  $\delta$ - $\text{Bi}_2\text{O}_3$  near band gap transitions. © 2012 American Institute of Physics. [<http://dx.doi.org/10.1063/1.4747198>]

Oxide materials with high values of ionic conductivity are a subject of increasing interest for potential applications in energy generation and storage technology. Bismuth trioxide ( $\text{Bi}_2\text{O}_3$ ) is a semiconductor with interesting physical properties, such as a wide optical band-gap, high refractive index and dielectric permittivity, good photoconductive response, and ionic conductivity, which make this material suitable for applications in solid oxide fuel cells, gas sensing, optical coatings, catalysis, and optoelectronics.<sup>1–3</sup>  $\text{Bi}_2\text{O}_3$  has four main polymorphs,<sup>4,5</sup> labeled as  $\alpha$  (monoclinic),  $\beta$  (tetragonal),  $\gamma$  (bcc), and  $\delta$  (fcc), with different physical properties.  $\alpha$ - $\text{Bi}_2\text{O}_3$  is stable from room temperature up to 730 °C. At 730 °C, this phase transforms into the  $\delta$ - $\text{Bi}_2\text{O}_3$  phase, which remains stable up to its melting point (825 °C).  $\beta$ - $\text{Bi}_2\text{O}_3$  and  $\gamma$ - $\text{Bi}_2\text{O}_3$  are obtained as metastable phases during the cooling of  $\delta$ - $\text{Bi}_2\text{O}_3$ . Below 640 °C approximately, these metastable phases are transformed into  $\alpha$ - $\text{Bi}_2\text{O}_3$ . The cubic  $\delta$ - $\text{Bi}_2\text{O}_3$  phase is one of the best oxygen ion conductors known ( $\sigma \sim 1.5 \text{ S cm}^{-1}$ ) and is considered as a reference material within the field of solid electrolytes.<sup>6</sup> This phase can be stabilized by addition of rare earth oxides, but the conductivity drops by about two orders of magnitude. In the past years,  $\delta$ - $\text{Bi}_2\text{O}_3$  thin films have been synthesized by electrodeposition and magnetron sputtering.<sup>7,8</sup> In the present work, we investigate the possibility to induce a local and permanent  $\alpha$ - $\text{Bi}_2\text{O}_3$  to  $\delta$ - $\text{Bi}_2\text{O}_3$  phase transformation in bulk materials as well as in nanowires by laser irradiation. The ability to locally modify the electrical conductivity and optical properties of a wide range of materials is of great interest for the development of sensing and storage applications. In this framework, local laser irradiation is a useful technique able to modify the structure, composition, and physical properties of several oxides,<sup>9–11</sup> chalcogenides,<sup>12</sup> and metallic alloys.<sup>13</sup> Laser irradiation of the  $\text{Bi}_2\text{O}_3$  samples was carried out by using a confocal microscope. The induced transformation was monitored *in situ* as a function of irradiation time and laser power by micro-Raman and photoluminescence (PL) spectroscopies.

Two kinds of  $\text{Bi}_2\text{O}_3$  samples were investigated in the present work, ceramics and nanowires (Fig. 1).  $\alpha$ - $\text{Bi}_2\text{O}_3$  ceramic samples were prepared following the procedure described in Ref. 14. In order to grow the nanowires, a mixture containing 80 wt. % Bi powder (Goodfellow, 99.997%) and 20 wt. %  $\text{Er}_2\text{O}_3$  powder (STREM, 99.9%) was compacted under compressive load to form disk-shaped samples of about 7 mm diameter and 1 mm thickness. These samples were then annealed at 800 °C for 4 h in a horizontal tube furnace under Ar flow. The treatment leads to the growth of a high density of single crystalline  $\alpha$ - $\text{Bi}_2\text{O}_3$  nanowires, as revealed by x-ray diffraction (XRD) and high-resolution transmission electron microscopy (HRTEM).<sup>15</sup> Energy dispersive x-ray microanalysis performed in scanning and transmission electron microscopes (SEM, TEM) did not detect the presence of Er in the  $\text{Bi}_2\text{O}_3$  nanowires. The addition of  $\text{Er}_2\text{O}_3$  alters the oxidation kinetics in the growth of the nanostructures, probably influencing the nucleation and oxidation process. Actually, nanowires were not obtained when similar treatments were carried out using pure Bi as the only precursor material, so that  $\text{Er}_2\text{O}_3$  was used here to favor the growth of these nanostructures.

The morphology of the samples before and after laser irradiation was investigated by using a FEI Inspect SEM. Micro-Raman and PL measurements were carried out at room temperature in a Horiba Jovin-Yvon LabRAM HR800 system. The samples were excited by a 325 nm He–Cd laser on an Olympus BX 41 confocal microscope with a 40 $\times$  objective. A charge coupled device detector was used to collect the scattered light dispersed by a 2400 lines/mm grating. The size of the laser spot on the sample was 2  $\mu\text{m}$  approximately. In order to adjust the applied power densities, the excitation light was attenuated by using neutral density filters. Both ceramics and nanowires were attached to the confocal microscope sample holder by using a conductive adhesive carbon tape.

Figure 1 shows SEM images of both kinds of samples prior to irradiation.  $\alpha$ - $\text{Bi}_2\text{O}_3$  ceramics show sintered grains with well defined grain boundaries and sizes in the (5–20)  $\mu\text{m}$  range. The investigated nanowires are (100–200) nm wide and up to 10  $\mu\text{m}$  long. In order to carry out the

<sup>a)</sup>e-mail: [cdiazgue@fis.ucm.es](mailto:cdiazgue@fis.ucm.es).

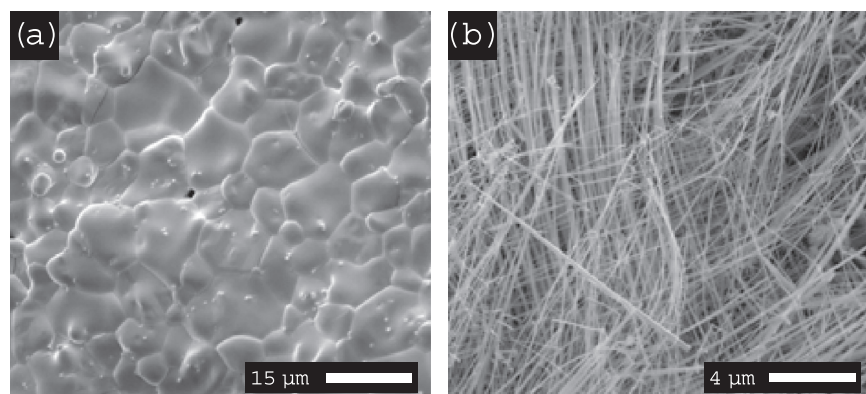


FIG. 1. SEM images of  $\alpha$ - $\text{Bi}_2\text{O}_3$  ceramics (a) and nanowires (b) prior to laser irradiation.

irradiation experiments, the nanowires were gently detached from the disk-shaped substrates. SEM observations of both kinds of samples after irradiation revealed no morphological changes irrespective of the power density used or the exposure time to the laser beam. The development of the  $\text{Bi}_2\text{O}_3$  structural change was monitored in ceramics and nanowires by Raman spectroscopy, using laser power densities ranging from  $10^5$  to  $10^2 \text{ W/cm}^2$  (Fig. 2). Spectra recorded at power densities below  $10^4 \text{ W/cm}^2$  show, in both kinds of samples, Raman bands peaked at about 212, 284, 315, 414, 447, and  $535 \text{ cm}^{-1}$ . These bands can be assigned to the  $\alpha$ - $\text{Bi}_2\text{O}_3$  phase

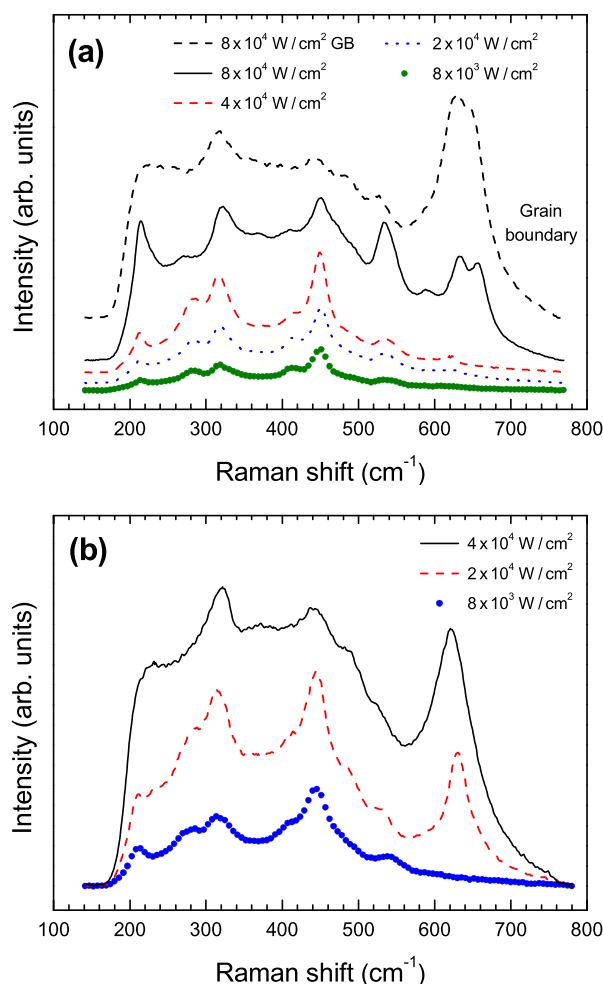


FIG. 2. Raman spectra, shifted for clarity, of  $\text{Bi}_2\text{O}_3$  ceramics (a) and nanowires (b) as a function of laser power density. Spectra shown in (a) were recorded at a grain interior unless otherwise indicated.

and are attributed to displacements of the O atoms with respect of the Bi atoms causing Bi-O elongation.<sup>16,17</sup> However, for power densities above  $2 \times 10^4 \text{ W/cm}^2$  in nanowires and approximately  $4 \times 10^4 \text{ W/cm}^2$  in ceramic samples, a new Raman band is observed peaked between  $619$  and  $628 \text{ cm}^{-1}$ . The intensity of this band increases by increasing the excitation density in all the investigated samples and is the dominant band in spectra recorded in irradiated grain boundaries of ceramic samples. These results evidence a laser-induced  $\alpha$  to  $\delta$  phase transformation during the irradiation of both  $\text{Bi}_2\text{O}_3$  ceramics and nanowires. Raman spectra of the  $\delta$ - $\text{Bi}_2\text{O}_3$  phase usually show a wide and asymmetric band centered between  $610$  and  $640 \text{ cm}^{-1}$ .<sup>7,8,18,19</sup> In the present case, the band characteristic of the  $\delta$  phase appears centered between  $619$  and  $625 \text{ cm}^{-1}$  in Raman spectra of the nanowires and between  $624$  and  $628 \text{ cm}^{-1}$  in those measured in ceramic samples.  $\delta$ - $\text{Bi}_2\text{O}_3$  may be regarded as an anion deficient fluorite structure, where Bi occupies the *fcc* sites, having a defect oxygen sublattice the structure of which is still under discussion. In fact, the oxygen sublattice is characterized by a complicated disorder, while there is still no clear understanding of the oxygen vacancies arrangement.<sup>20</sup> Moreover, the  $\delta$  phase is likely to involve a thermal average of a range of different local environments.<sup>21</sup> This structural disorder may account for the somewhat different peak frequencies of the  $\delta$ - $\text{Bi}_2\text{O}_3$  Raman band found in nanowires and ceramics. Raman bands characteristic of  $\alpha$ - $\text{Bi}_2\text{O}_3$  can still be observed in the Raman spectra of the strongly irradiated areas, suggesting that this thermally driven process probably takes place in the central part of the area irradiated by the laser spot, where temperature reaches its highest value due to the Gaussian intensity profile of the laser beam. The temperature distribution is less homogeneous in bulk material than in nanowires due to the existence of grain boundaries and other extended defects. Moreover, the size of the laser spot is much smaller than the size of the polycrystalline samples, which is not the case for the irradiated nanowires. This may explain the occasional appearance of a Raman peak at about  $656 \text{ cm}^{-1}$  only in spectra from irradiated ceramics, in agreement with Raman observations reported by Fan *et al.*<sup>18</sup> in annealed  $\delta$ - $\text{Bi}_2\text{O}_3$ . These authors tentatively attributed a Raman peak centered at  $655 \text{ cm}^{-1}$  to the metastable  $\gamma$ - $\text{Bi}_2\text{O}_3$  phase by comparison of XRD and Raman measurements.

Transformation kinetics was investigated *in situ* in both ceramics and nanowires by irradiating the samples with power densities above the previously mentioned threshold



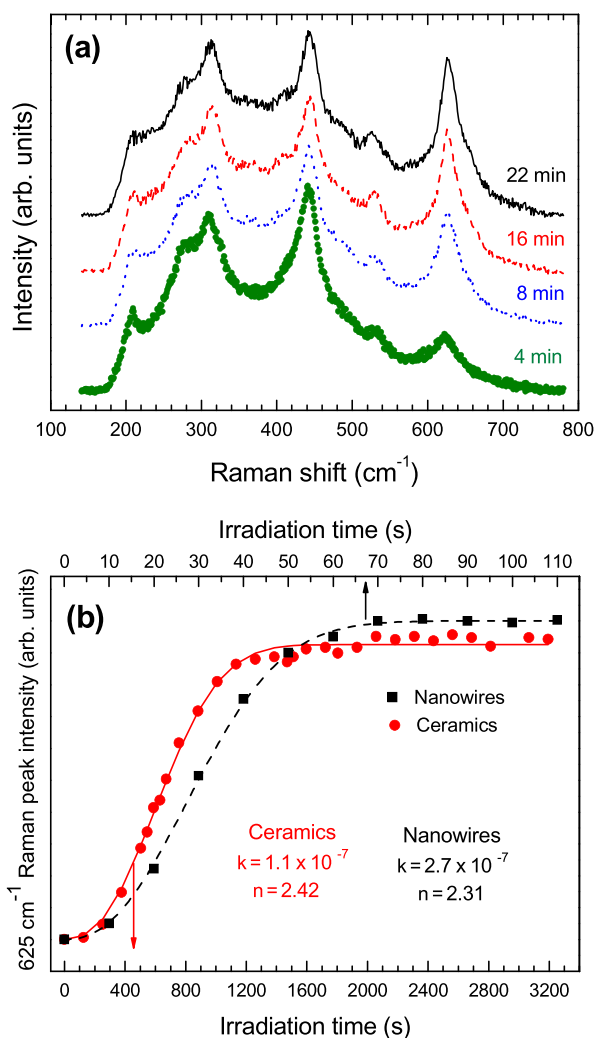


FIG. 3. (a) Raman spectra of  $\text{Bi}_2\text{O}_3$  ceramics after different irradiation times. (b) Temporal intensity evolution of the  $625\text{ cm}^{-1}$  Raman peak in ceramic samples and nanowires. Dots correspond to experimental data while solid lines correspond to fits to the JMA model. Data correspond to power densities of  $8 \times 10^4\text{ W/cm}^2$  (ceramics) and  $4 \times 10^4\text{ W/cm}^2$  (nanowires).

values and collecting Raman spectra at fixed time intervals. Fig. 3(a) shows spectra of  $\text{Bi}_2\text{O}_3$  ceramics irradiated for different times. A progressive increase of the relative intensity of the band centered near  $625\text{ cm}^{-1}$ , characteristic of the  $\delta\text{-Bi}_2\text{O}_3$  phase, is observed by increasing the exposure time to the laser beam. After approximately 20 min of laser irradiation, the intensity of the mentioned band reaches a saturation value [Fig. 3(b)]. A similar behavior is observed for nanowires, but the transformation takes place much faster. Actually, saturation is reached just 1 min after irradiation started. The observed thermal conductivities of oxide nanostructures are frequently lower than the corresponding bulk values, which is mainly attributed to an increased phonon-boundary scattering rate.<sup>22</sup> Such behavior is in agreement with our Raman measurements, since the threshold power density required to trigger the  $\alpha$  to  $\delta$  phase transformation is lower for nanowires than for ceramics, while saturation of the  $625\text{ cm}^{-1}$  band is reached faster in nanowires than in ceramics.

The temporal intensity evolution of the  $625\text{ cm}^{-1}$  Raman signal of both kinds of samples is plotted in Fig. 3(b).

Assuming that the intensity of such band is proportional to the volume of transformed material,<sup>9</sup> from  $\alpha\text{-Bi}_2\text{O}_3$  to  $\delta\text{-Bi}_2\text{O}_3$ , the experimental data were fitted to the Johnson-Mehl-Avrami (JMA) equation:<sup>23</sup>

$$X = 1 - \exp(-Kt^n).$$

This model, originally proposed to describe crystallization kinetics for isothermal annealing conditions, has been frequently applied to describe phase transformation induced by laser irradiation in different materials.<sup>9,24</sup>  $X$  represents the transformed volume fraction in the irradiated area,  $K$  is an effective rate constant and the Avrami exponent,  $n$ , is related to the nucleation rate and/or the growth morphology. The obtained values, 2.3 for nanowires and 2.4 for ceramics, suggest that crystallization proceeds by a diffusion-controlled growth mode with nearly constant nucleation rate.<sup>25</sup> The disorder characteristic of  $\delta\text{-Bi}_2\text{O}_3$  can be structurally derived from the  $\alpha$  phase. As a consequence of the growing degree of oxygen site disorder with increasing temperature, the oxygen sublattice exhibits a liquid-like behavior which promotes higher oxygen ion diffusion only when a certain degree of the structural disorder is achieved, mimicking a process which is analogous to a pre-melting phenomenon.<sup>26</sup>

The time stability of the laser induced  $\delta\text{-Bi}_2\text{O}_3$  phase was investigated for both types of samples. In order to do that, ceramics and nanowires were irradiated with laser power densities above their respective threshold values and for times longer than the saturation values shown in Fig. 3(b). Precisely, nanowires were irradiated during 90 s and ceramics during 20 min by using a power density of  $8 \times 10^4\text{ W/cm}^2$ . Raman spectra were recorded before beginning irradiation and at different time lapses after the end of irradiation, using, in all cases, a low laser power density of  $8 \times 10^3\text{ W/cm}^2$ . The absence of Raman bands above  $600\text{ cm}^{-1}$  before irradiation and its presence 2 h after irradiation (Fig. 4) reveal the stability of the induced  $\delta\text{-Bi}_2\text{O}_3$  phase. Actually, an intensity decrease of the mentioned

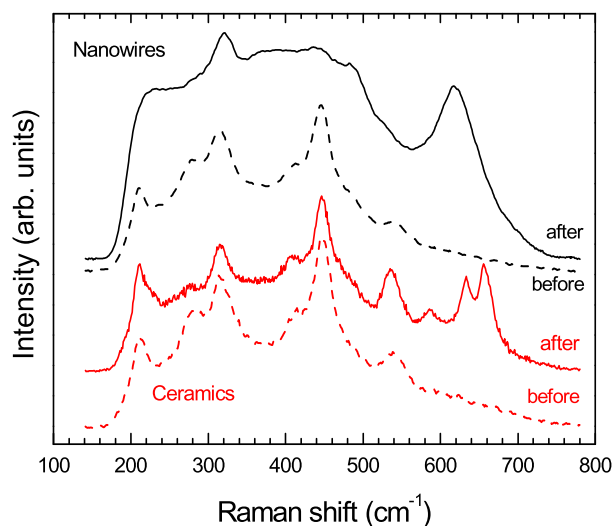


FIG. 4. Raman spectra of ceramics and nanowires before and 2 h after laser irradiation. Nanowires were irradiated during 90 s and ceramics during 20 min by using a power density of  $8 \times 10^4\text{ W/cm}^2$  in both cases. Spectra were recorded by using a laser power density of  $8 \times 10^3\text{ W/cm}^2$ .

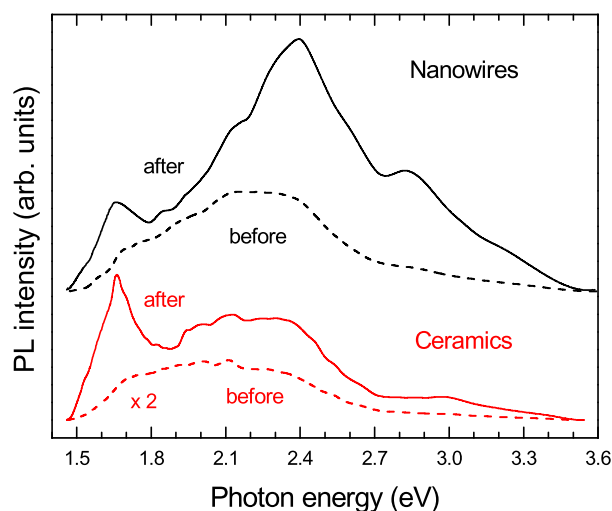


FIG. 5. PL spectra of ceramics and nanowires before and 2 h after laser irradiation. Irradiation was carried out by using a power density of  $8 \times 10^4 \text{ W/cm}^2$ . Spectra shown in this figure were recorded by using a laser power density of  $8 \times 10^3 \text{ W/cm}^2$ .

Raman signal with time was neither observed in nanowires nor in ceramic samples after finishing the corresponding irradiation periods.

The appearance of the  $\delta$  phase was also monitored by PL spectroscopy. Besides emission in the (3.20–2.85) eV range, usually attributed to band gap transitions, PL emission in the visible range has been frequently attributed in  $\alpha\text{-Bi}_2\text{O}_3$  to radiative transitions involving Bi ions with different charge states.<sup>14,27–29</sup> Figure 5 shows PL spectra of our bismuth oxide ceramics and nanowires before and after laser irradiation. A broad, complex, emission peaked between 2.4 and 2.0 eV can be observed before irradiation in all the samples investigated. Laser irradiation enhances PL intensity and induces significant changes in the spectral distribution of the emission. In particular, a dominant band peaked near 2.41 eV, with well resolved shoulders at 2.82 eV and 2.21 eV, can be clearly appreciated in spectra from the irradiated nanowires. Emission in the (3.1–2.2) eV spectral range has usually been attributed to  $\text{Bi}^{3+}$  intraionic transitions or charge transfer transitions between oxygen ligands and  $\text{Bi}^{3+}$  ions<sup>14,27,28</sup> in  $\alpha\text{-Bi}_2\text{O}_3$ , while luminescence bands in the (2.10–1.87) eV range were commonly assigned to  $\text{Bi}^{2+}$  intraionic transitions.<sup>14,29</sup> Furthermore, laser irradiation gives rise—in PL spectra of ceramics and nanowires—to an intense band centered at 1.67 eV, not observed in samples with the  $\alpha\text{-Bi}_2\text{O}_3$  structure. This band can be tentatively attributed to  $\delta\text{-Bi}_2\text{O}_3$  near band gap transitions. Actually, such emission appears only in the PL spectra of strongly irradiated areas, where the corresponding Raman spectra reveal the formation of the  $\delta$  phase. In addition, the peak energy of the mentioned PL band is very close to the band gap value of 1.73 eV measured by optical absorption in  $\delta\text{-Bi}_2\text{O}_3$  thin films<sup>8</sup> and is in agreement with recent theoretical calculations.<sup>30</sup>

In summary, an  $\alpha\text{-Bi}_2\text{O}_3$  to  $\delta\text{-Bi}_2\text{O}_3$  phase transformation can be locally induced by laser irradiation in ceramic samples and single crystal nanowires of this oxide, which may be of interest for electronic and optoelectronics applica-

tions due to the different conductivity and optical properties of such polymorphs. A threshold power density for the irradiation induced phase transformation of  $2 \times 10^4 \text{ W/cm}^2$  in nanowires and approximately  $4 \times 10^4 \text{ W/cm}^2$  in ceramic samples was determined by  $\mu$ -Raman spectroscopy in a confocal microscope. Transformation kinetics can be described by the Johnson-Mehl-Avrami equation. The time stability of this laser induced phase transformation was also established. Irradiation induces changes in the luminescence emission of both ceramics and nanowires. A PL emission band peaked near 1.67 eV, not observed in  $\alpha\text{-Bi}_2\text{O}_3$ , is tentatively attributed to  $\delta\text{-Bi}_2\text{O}_3$  near band gap transitions.

This work was supported by MICNN through projects MAT2009-07882 and CSD2009-0013.

- <sup>1</sup>A. Cabot, A. Marsal, J. Arbiol, and J. R. Morante, *Sens. Actuators B* **99**, 74 (2004).
- <sup>2</sup>A. Hameed, T. Montini, V. Gombac, and P. Fornasiero, *J. Am. Chem. Soc.* **130**, 9658 (2008).
- <sup>3</sup>L. Leontie, M. Caraman, M. Delibas, and G. I. Rusu, *Mater. Res. Bull.* **36**, 1629 (2001).
- <sup>4</sup>H. A. Harwig, *Z. Anorg. Allg. Chem.* **444**, 151 (1978).
- <sup>5</sup>H. A. Harwig and J. W. Weenk, *Z. Anorg. Allg. Chem.* **444**, 167 (1978).
- <sup>6</sup>N. M. Sammes, G. A. Tompsett, H. Näfe, and F. Aldinger, *J. Eur. Ceram. Soc.* **19**, 1801 (1999).
- <sup>7</sup>N. V. Skorodumova, A. K. Jonsson, M. Herranen, M. Strømme, G. A. Niklasson, B. Johansson, and S. I. Simak, *Appl. Phys. Lett.* **86**, 241910 (2005).
- <sup>8</sup>H. T. Fan, X. M. Teng, S. S. Pan, C. Ye, G. H. Li, and L. D. Zhang, *Appl. Phys. Lett.* **87**, 231916 (2005).
- <sup>9</sup>M. A. Camacho-López, L. Escobar-Alarcón, M. Picquart, R. Arroyo, G. Córdoba, and E. Haro-Poniatowski, *Opt. Mater.* **33**, 480 (2011).
- <sup>10</sup>H. L. Ma, J. Y. Yang, Y. Dai, Y. B. Zhang, B. Lu, and G. H. Ma, *Appl. Surf. Sci.* **253**, 7497 (2007).
- <sup>11</sup>P. F. Yan, K. Du, and M. L. Sui, *Acta Mater.* **58**, 3867 (2010).
- <sup>12</sup>J. Siegel, A. Schropp, J. Solís, C. N. Afonso, and M. Wuttig, *Appl. Phys. Lett.* **84**, 2250 (2004).
- <sup>13</sup>A. J. Birnbaum, G. Satoh, and Y. L. Yao, *J. Appl. Phys.* **106**, 043504 (2009).
- <sup>14</sup>M. Vila, C. Díaz-Guerra, and J. Piqueras, *Mater. Chem. Phys.* **133**, 559 (2012).
- <sup>15</sup>See supplementary material at <http://dx.doi.org/10.1063/1.4747198> for XRD and HRTEM of the grown nanowires.
- <sup>16</sup>R. J. Betsch and W. B. White, *Spectrochim. Acta, Part A* **34**, 505 (1978).
- <sup>17</sup>V. N. Denisov, A. N. Ivlev, A. S. Lipin, B. N. Mavrin, and V. G. Orlov, *J. Phys. Condens. Matter* **9**, 4967 (1997).
- <sup>18</sup>H. T. Fan, S. S. Pan, X. M. Teng, C. Ye, and G. H. Li, *J. Phys. D: Appl. Phys.* **39**, 1939 (2006).
- <sup>19</sup>A. Rubbens, M. Drache, P. Roussel, and J. P. Wignacourt, *Mater. Res. Bull.* **42**, 1683 (2007).
- <sup>20</sup>M. Yashima and D. Ishimura, *Chem. Phys. Lett.* **378**, 395 (2003).
- <sup>21</sup>C. E. Mohn, S. Stølen, S. T. Norberg, and S. Hull, *Phys. Rev. B* **80**, 024205 (2009).
- <sup>22</sup>L. Shi, Q. Hao, C. Yu, N. Mingo, X. Kong, and Z. L. Wang, *Appl. Phys. Lett.* **84**, 2638 (2004).
- <sup>23</sup>M. Avrami, *J. Chem. Phys.* **7**, 1103 (1939); **8**, 212 (1940); **9**, 177 (1941).
- <sup>24</sup>G. Mannino, C. Spinella, R. Ruggeri, A. La Magna, G. Fiescaro, E. Fazio, F. Neri, and V. Privitera, *Appl. Phys. Lett.* **97**, 022107 (2010).
- <sup>25</sup>S. Venkataraman, H. Hermann, C. Mickel, L. Schultz, D. J. Sordellet, and J. Eckert, *Phys. Rev. B* **75**, 104206 (2007).
- <sup>26</sup>L. E. Depero and L. Sangaletti, *J. Solid State Chem.* **122**, 439 (1996).
- <sup>27</sup>L. Kumari, J.-H. Lin, and Y.-R. Ma, *Nanotechnology* **18**, 295605 (2007).
- <sup>28</sup>V. Babin, V. Gorbenko, A. Krasnikov, A. Makhov, M. Nikl, K. Polak, S. Zazubovich, and Y. Zorenko, *J. Phys.: Condens. Matter* **21**, 415502 (2009).
- <sup>29</sup>M. Gaft, R. Reisfeld, G. Panczer, G. Boulon, T. Saraidarov, and S. Erlich, *Opt. Mater.* **16**, 279 (2001).
- <sup>30</sup>A. Matsumoto, Y. Koyama, and I. Tanaka, *Phys. Rev. B* **81**, 094117 (2010).